

Sources of Errors in Structured Light 3D Scanners

Prem Rachakonda, Bala Muralikrishnan, Daniel Sawyer

Dimensional Metrology Group,

Sensor Science Division,

National Institute of Standards and Technology, Gaithersburg, MD

1 INTRODUCTION

The Dimensional Metrology Group (DMG) at the National Institute of Standards and Technology (NIST) has been involved in the development of documentary standards for a variety of 3D metrology instruments such as coordinate measuring machines (CMMs), laser trackers and terrestrial laser scanners (TLSs). As a US National Metrology Institute (NMI), NIST develops procedures to evaluate dimensional metrology instruments in an unbiased and objective manner. Lately, several of DMG's industry partners have shown interest in Structured Light (SL) scanners and have expressed the need to characterize the instrument performance.

Structured light scanners are portable short-range 3D imaging systems that use patterns of projected images or light patterns to measure an object. These scanners have very few or no moving components and capture millions of points on surfaces of an object in their field of view. SL scanners build on classical photogrammetry techniques and project encoded images on an object, which add texture to the object and simplify the correspondence problem, i.e., corresponding points in the projected and the captured images. The precision and accuracy of measurements from SL scanners can be appropriate for certain industrial applications such as reverse engineering, quality control, and biometrics. These scanners also have faster data acquisition rates and are relatively inexpensive compared to the large stationary CMMs. This makes them suitable for applications that do not need the low uncertainties typical of CMMs or those that require in situ measurements.

SL scanners have been commercially available for over a decade and some commercial scanners are evaluated using one of two German guidelines – VDI/VDE* 2634 parts 2 and/or 3 [1,2]. Several other research groups and NMIs have developed physical artifacts that are agnostic to instrument construction and are purpose driven. The use of such guidelines and artifacts is not well understood for instruments which have a variety of sensor configurations, projected patterns, sensor/work volumes, point densities, triangulation angles and targets of varying size & form. It is also not clear if these guidelines/artifacts are sensitive to all the sources of errors that are present in these systems. The two VDI/VDE 2634 guidelines for evaluating the performance of the SL scanners use artifacts of known mechanical and optical characteristics, but the real-world usage of these scanners may involve objects of varying characteristics. The end user may not be able to make informed decisions if an instrument is specified based on these guidelines/standards but is used for an application that deviates from the test conditions. This can cause an enormous financial burden for organizations that intend to invest in the technology, but do not have appropriate standards to aid in selecting an instrument that meets their needs.

In this context, this paper will describe the ongoing activities at NIST to study various sources of errors in SL scanners with an objective of characterizing their performance. The paper will first give some background information on the principle of operation of SL scanners, the state-of-the-art of documentary standards/artifacts and describe some scanners available to the authors. The paper will then discuss the various sources of errors in SL scanners that influence their

* German: Verein Deutscher Ingenieure/Verband der Elektrotechnik (English: Association of German Engineers/Association of Electrical Engineering)

measurements and describe a few experiments that were performed to understand some of these errors.

2 PRINCIPLE OF OPERATION

Structured light scanners are systems that acquire 3D coordinates of points on surfaces of an object using the principle of triangulation. These scanners project a pattern of light on an object, capture the distorted patterns from the object using a camera and calculate the 3D coordinates. The principle of triangulation used to calculate the depth of the projected points on the object is based on the knowledge of the distance between the pattern projector and the camera and the angle between them with respect to a location on the object.

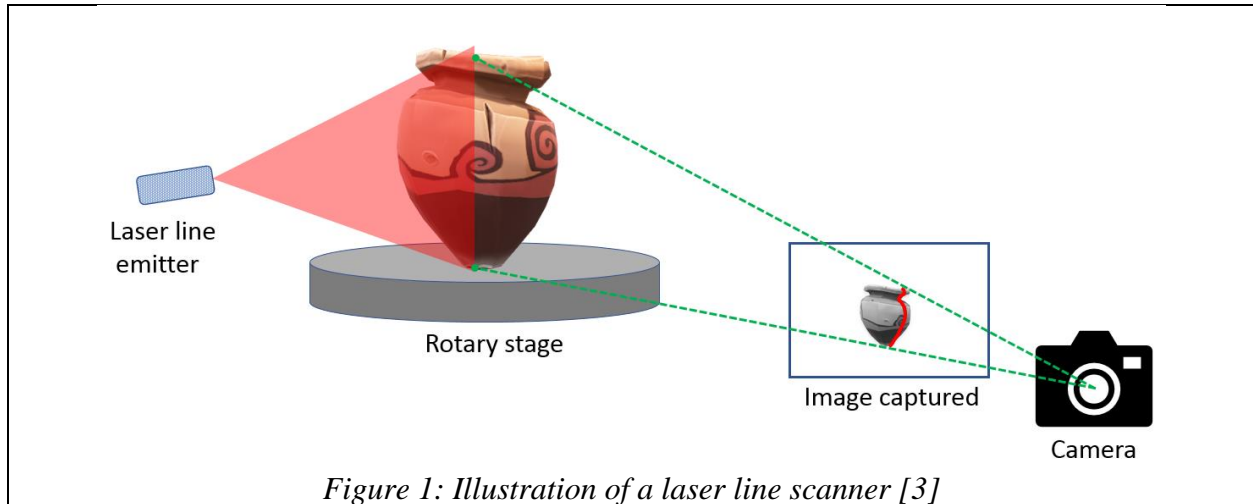


Figure 1: Illustration of a laser line scanner [3]

To explain the principle of operation of an SL scanner, we will first explain the principle of a laser line scanner, which also uses the principle of triangulation. A laser line scanner has a laser line emitter that projects a plane of light on to an object, and a camera that captures the distorted image of the line corresponding to the object's contour (see Figure 1). To obtain a complete 3D scan, such a scanner needs the object to move relative to the laser line. For example, the object can be mounted on a linear or rotary stage and moved relative to the scanner or an opto-mechanical system may be used to sweep the laser line over the object to obtain a 3D scan.

A structured light scanner uses the same principle, but instead of a laser line emitter, it uses a projector to illuminate the object (see Figure 2). The purpose of the projector is to "paint" the object with a known pattern that can be easily captured using a camera. However, to detect these patterns from the image, common edge/line detection algorithms are not enough. Any illumination change will result in loss of data or detection of lines at a wrong location. To address this issue, a structured light scanner uses a projector to display lines in several patterns or colors (structured light) to "paint" the object.

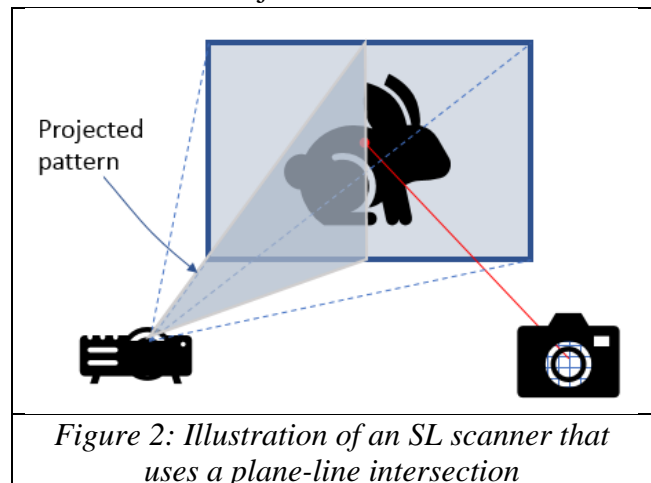


Figure 2: Illustration of an SL scanner that uses a plane-line intersection

There are several coding techniques for reducing the error of detecting the lines from the captured images. This is possible because modern projectors are capable of projecting 1920 lines for a high-

definition (HD) projector and 3840 lines for a 4K projector, where the number of lines correspond to the projector's columns in pixels.

The purpose of a coded light pattern/image is to easily differentiate between two lines in the distorted image as captured by the camera. For example, the first column of the projected image could be red, and the next column could be yellow and so on. And, like a laser line scanner, the triangulation principle is used to recover the depth information.

While discussing structured light scanners, it is important to mention one other widely used technique – photogrammetry, and specifically stereophotogrammetry, which also uses the triangulation principle. Photogrammetry based instruments are considered passive vision imaging systems that rely on the distinct features in the scene to obtain the correspondence between the images in two or more cameras or multiple images from the same camera from multiple positions. When such features do not exist, the instrument fails to perform the triangulation adequately. For example, measuring the form of the painted exterior of an automobile with a slight dent will be challenging using photogrammetry [4]. On the other hand, structured light scanners are considered active vision scanners and use known image patterns to achieve correspondence between the projected image and the captured image.

3 STATE-OF-THE-ART OF PERFORMANCE EVALUATION STANDARDS

Common specifications and/or common procedures to evaluate scanners will help the end users and decision makers in choosing the right scanner for their application. Scanners may be evaluated in many ways, one of which is to develop a set of procedures that use artifacts of common geometry such as planes, spheres and cones. Another way is to develop specific reference artifacts with complex geometry and corresponding procedures that encompass the application requirements. Whichever method is used to characterize a scanner, it should be acceptable to both users and manufacturers of SL scanners. The next sub-sections will discuss some of the existing methods to characterize optical 3D scanners such as SL scanners.

3.1 Reference artifacts

The National Research Council of Canada (NRC) and the National Physical Laboratory of United Kingdom (NPL) are the NMIs of their respective countries and have been working for several years on developing artifacts [5,6,7] shown in Figure 3 and Figure 4 for short-range optical 3D scanners. Though the use of these artifacts has not been adopted yet by any documentary



Figure 3: NRC artifact [6]



Figure 4: NPL artifact [7]

standard, they provide a way for end-users to characterize their instrument. Many organizations also develop task specific artifacts and/or procedures to address their internal needs.

3.2 Documentary standards

As of the writing of this paper, there are no international documentary standards for SL scanners. There are two German guidelines[†] that are used to evaluate some SL scanners, namely the VDI/VDE 2634 Parts 2 and 3. These two guidelines were written as an extension of the International Standards Organization (ISO) 10360 standards for CMMs, instruments whose operating principles are much different than those of SL scanners [6]. In 2018, the ISO Technical Committee (TC) 213 initiated standards development work on a Part 13 to the ISO 10360 series that addresses the evaluation of SL scanners. Thus far, this part includes some of the procedures of the VDI/VDE 2634 guidelines, along with more exhaustive testing on the number of points and point filtering criteria. Since this document is still under development, its discussion is out of the scope of this paper.

<i>Table 1: Comparison of the two VDI/VDE 2634 guidelines</i>		
	VDI-VDE 2634 Part 2 (2012)	VDI-VDE 2634 Part 3 (2008)
Multiple views	No	Yes
Filtering of points	Limited specification on point rejection	
	Probing errors	
Artifact	Sphere	Sphere
Sphere diameter*	$0.02L_0$ to $0.2L_0$	$0.02L_s$ to $0.2L_s$
Positions	10	≥ 3
Scans/position	1	≥ 5
Quality parameter	Error in sphere form	Error in sphere form
	Error in sphere diameter	Error in sphere diameter
	Sphere spacing errors	
Artifact	Like a dumbbell	Like a dumbbell
Sphere diameter*	$0.02L_0$ to $0.2L_0$	$0.02L_s$ to $0.2L_s$
Dumbbell length*	$\geq 0.3L_0$	Varies
Positions	7	7
Scans/position	1	1
Quality parameter	Error in sphere-sphere distance	Error in sphere-sphere distance
	Flatness measurement error	Length measurement error
Artifact	Flat plate	Ball bar/ball plate/gage blocks
Artifact width	Minimum 50 mm	N/A
Artifact length*	Minimum $0.5 * L_0$	$0.02L_s$ to $0.2L_s$
Positions	≥ 6	7
Scans/position	1	1
Quality parameter	Flatness measurement error	Error in artifact length

* A dumbbell can be replaced by two spheres separated by a rigid mount.

[†] Though guidelines are informative, these documents are considered as *de facto* standards by the practitioners. There exists a VDI/VDE 2634 Part 1, but it is not applicable to imaging systems based on area scanning, like SL scanners.

The two VDI/VDE guidelines mentioned here use simple geometries such as spheres in multiple positions and orientations to evaluate optical scanners. One of the major differences between the two VDI/VDE guidelines is that Part 2 is applicable for scanners that produce area scans based on a single view and Part 3 is applicable for scanners using multiple views that extends the measurement volume. Table 1 provides a more detailed comparison of the two guidelines. In this table, L_s is the length of sensor measuring volume diagonal and L_0 is the body/spatial diagonal of the measuring volume, both of which are specified by the manufacturer.

There are several areas where these two guidelines are not adequate for choosing SL scanners today. These two guidelines do not address all the scanner configurations that are currently available, nor provide all the parameters that describe the performance of a scanner. Below are some of the issues in these two guidelines that could be improved.

- a) The VDI/VDE guidelines do not recommend any tests to determine the scanner's resolution in the X, Y, Z axes for a user to determine the minimum size of a feature that can be measured by the scanner. Some scanners offer a theoretical lateral resolution (X, Y) based on the camera sensor's pixels and the field of view, which does not indicate the smallest feature that can be distinguished.
- b) VDI/VDE 2634 Part 3 does not require the calculation of the flatness measurement error, whereas it is required by Part 2.
- c) Accuracy values of these instruments vary based on the location of the artifact and/or distance of the artifact from the scanner. A single accuracy value may not be adequate for the end user.
- d) Recommended artifact geometries are either flat or convex (spheres). The performance of some of these scanners was found to be different for concave surfaces, especially when scanning deep, dark and/or shiny features.
- e) The guidelines are unclear for merged 3D scans obtained using different scanner settings to capture the surface without any relative displacement between the scanner and the object. Such scans are typically needed when the object is dark and/or shiny and are obtained by merging scans at various exposure, gain or aperture settings.
- f) The guidelines are also not clear when the scanner uses multiple cameras and generates scan data by merging the scans from multiple cameras.
- g) Both the VDI/VDE guidelines do not have a specification on the number of points to consider. Point densities affect the error in calculating the quality parameters.
- h) Both the VDI/VDE guidelines have criteria for rejecting a certain percentage of points, but do not have a prescribed method to reject those points.

4 STRUCTURED LIGHT SCANNERS

There are several configurations of structured light scanners that are commercially available, and a discussion of the various scanners and their features is beyond the scope of this paper. Some of these scanners are priced from \$100 to \$200K, with various hardware & software options and performance characteristics. The price of the instruments may not correlate well with their performance, but it is important to note that the same principle is used in products for various applications at various price ranges. SL scanners may use different coding patterns, hardware, filters and proprietary algorithms. DMG procured three commercial structured light scanners to study their construction and performance.

Table 2: Types of scanners used by DMG

Name	SK	SE	SA	SC
Application	Gaming	Hobby	Industrial	Experimental
# of cameras	1	1	2	1
Camera Resolution	0.3MP	1.3MP	8MP	2MP
Projector type	LED pattern	LED lamp	LED lamp	Metal halide lamp
Light color	Infrared	White	Blue	Multi-color
Light pattern	Pseudo random binary dots	Hybrid	Gray/binary code	Gray code
Projector resolution	N/A	<2 MP	28MP	2 MP
Single scan volume	$\approx 2 \text{ m}^3$	$\approx 1.73 \text{ m}^3$	$\approx 0.11 \text{ m}^3$	$\approx 2 \text{ m}^3$
Stated accuracy	NA	<0.050 mm	0.032 mm	N/A

There are also several implementations of structured light scanners in open literature including open source software. DMG researchers built an SL scanner (scanner SC) based on the design and software described by Taubin et al [8] that uses a plane-line intersection as illustrated in Figure 2. Some of the specifications of these four scanners are given in Table 2 and the scanner SC will be described next.

4.1 Custom-built 3D scanner

The purpose of building a 3D structured light scanner was to enable the authors to modify all the parameters that affect the instrument performance – a capability that was limited by commercial instruments. Even though commercial scanners resulted in higher quality scans than this custom scanner, the ability to modify the instrument parameters is very useful in understanding the instrument error sources.

The hardware for the custom-built SL scanner includes a commercial off-the-shelf projector (Optoma HD 143X), a webcam (Microsoft LifeCam Studio) both of which have a resolution of 1920 pixels \times 1080 pixels and shown in Figure 5a. The software was a pre-compiled binary of the C++ code developed by Taubin et al [8]. This scanner uses a series of temporal gray code patterns as shown in Figure 6. The software also has a projector-camera calibration routine and a scanning routine that generates 3D point cloud data. Figure 6 and Figure 7 show a picture of the artifacts being scanned and the 3D data respectively using the webcam.

After this initial build, the webcam was replaced by a digital single lens reflex (DSLR) camera (Canon T1i, shown in Figure 5b) to improve the performance of the scanner. A third-party commercial software was used to convert the DSLR to a UVC (USB video class) compatible camera. This additional software enabled a simpler software integration, instead of modifying the C++ code that only worked with UVC webcams. The DSLR camera provided a way to control the camera parameters much more easily than what a consumer grade webcam would allow. It also allowed the usage of a higher resolution images, larger sensor size and higher quality lenses

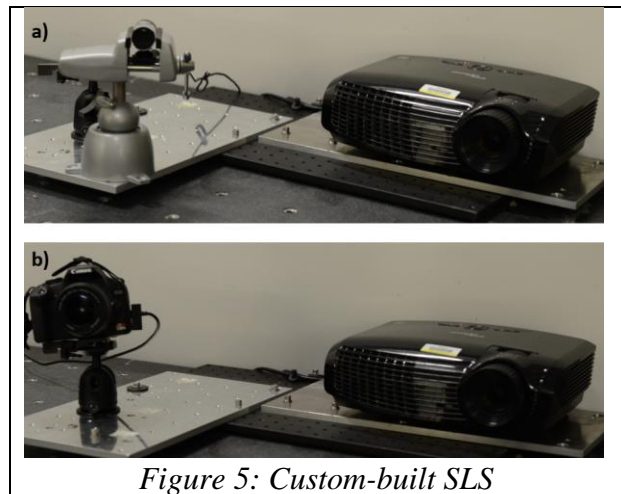


Figure 5: Custom-built SLS

resulting in images with higher signal-to-noise ratios. It should be noted that higher camera pixel resolution is different from the resolving power of the lens, i.e., its ability to differentiate two lines as separate.

5 PARAMETERS THAT AFFECT SCANNER PERFORMANCE (ERROR SOURCES)

Measurements obtained by structured light scanners are affected by several parameters. These parameters are the sources of errors in these scanners. In commercial instruments, many of the error sources are addressed using higher quality hardware, optics, rigid mounting, and hardware/software filters. Error sources can be categorized as caused by a) scanner construction, b) target construction, c) environment, d) operating modes/settings and e) data acquisition and post-processing. These error sources are described in detail in the following sub-sections.

5.1 Errors due to scanner construction

5.1.1 Calibration (intrinsic and extrinsic) and distortion parameters

SL scanners need to be calibrated before they can be used for measurement. This calibration process typically uses an artifact with a grid of known 2D patterns and will result in the calculation of calibration parameters. The methods used in performing calibration are described next.

a) Camera calibration

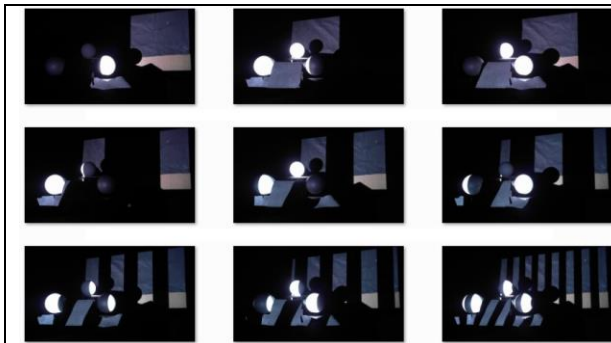


Figure 6: The first nine sequences of the gray code pattern used by the custom-built SLS

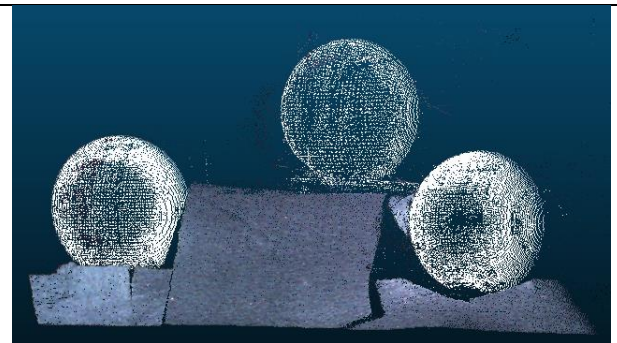


Figure 7: 3D scan of three spheres scanned using a custom-built SLS

Camera calibration has been studied extensively [9,10,11,12] and is well understood in the field of computer vision. It is described in this paper in brief because the parameters that affect camera calibration also affect the structured light scanner calibration. Cameras used for SL scanners are calibrated based on a general projective camera model [11] and it is a generalized model of a pinhole camera. It requires the determination of five intrinsic parameters and six extrinsic parameters of a camera.

The calibration process based on this model is valid only for undistorted images, as a pinhole camera does not use any lens. So, the first step in this calibration process is to generate an undistorted image by minimizing the radial and tangential distortions due to the camera lens illustrated in Figure 9 and Figure 10 respectively. This involves the calculation of typically three parameters (k_1, k_2, k_3) for radial distortion and two parameters (p_1, p_2) for tangential distortion[‡].

[‡] The calibration routine described in this paper, MATLAB and the open source computer vision library (OpenCV) use different notations for the matrices and the distortion parameters. The parameters described here are per OpenCV.

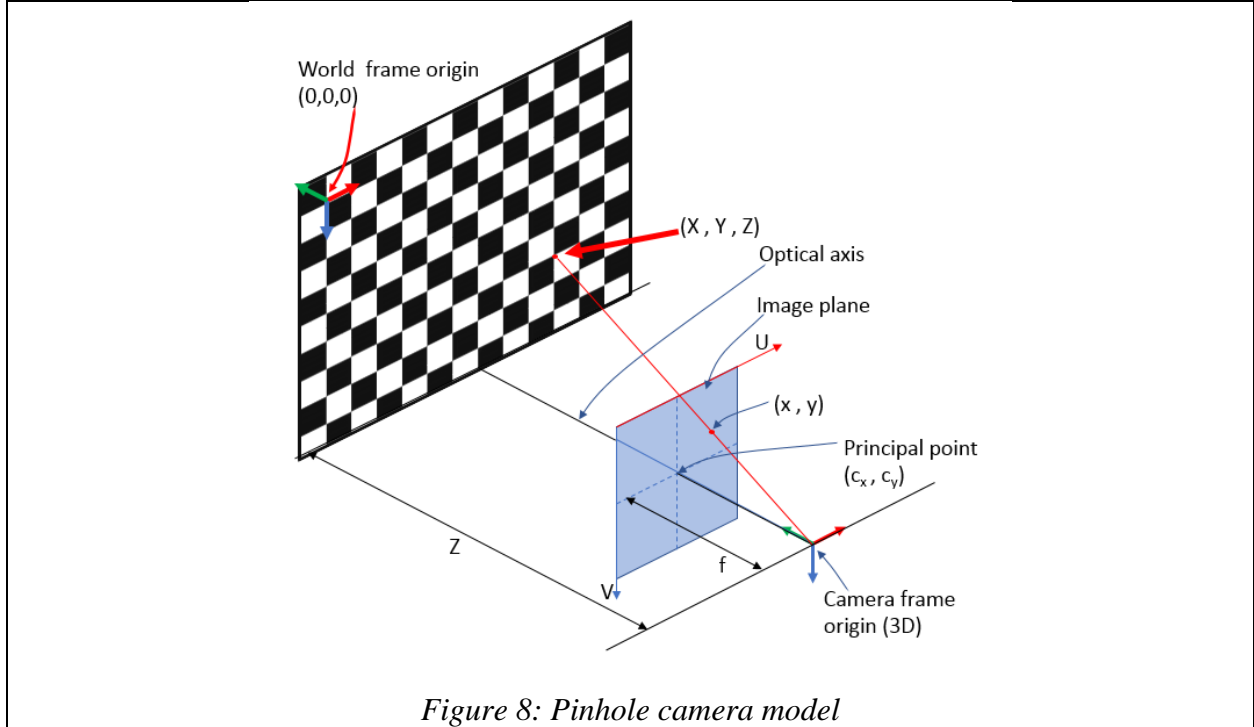


Figure 8: Pinhole camera model

The relationship between the 2D image points captured by the camera and the 3D world points is given by equation 1. Here X represents the world coordinates of a point $[X, Y, Z, 1]^T$, x represents the undistorted image coordinates $[u, v, 1]^T$, R is a 3×3 rotation matrix, t is a 3×1 translation matrix and K represents a 3×3 intrinsic matrix of a camera. The rotation and translation matrices represent the relationship between the origin of the world points (typically set arbitrarily on the calibration artifact) and the camera's origin as shown in Figure 8.

The camera's intrinsic matrix K is given by equation 2, which is composed of five intrinsic parameters. These are, the focal lengths f_x, f_y , the optical center or principal point in two orthogonal directions c_x, c_y and axis skew s .

$$x = K[R \ t]X. \tag{1}$$

The skew coefficient (s) is to account for any non-orthogonality in the image axes (non-rectangular pixels). Typically, a pinhole camera model doesn't have this issue of skew but can be a result of certain digital conversion operations. The two focal lengths f_x, f_y are to account for rectangular pixels and are calculated from the physical focal length (F) in mm and the size of pixels m_x, m_y respectively in the units of pixels/mm [11]. That is, $f_x = F \times m_x$ and $f_y = F \times m_y$.

$$K = \begin{bmatrix} f_x & s & c_x \\ 0 & f_y & c_y \\ 0 & 0 & 1 \end{bmatrix}. \tag{2}$$

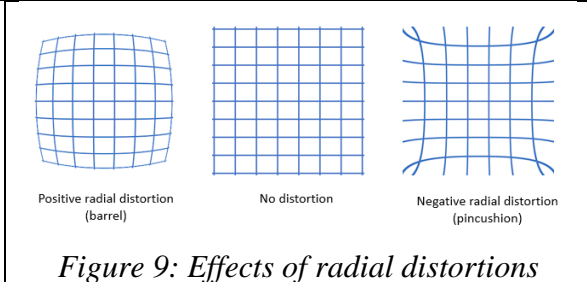


Figure 9: Effects of radial distortions

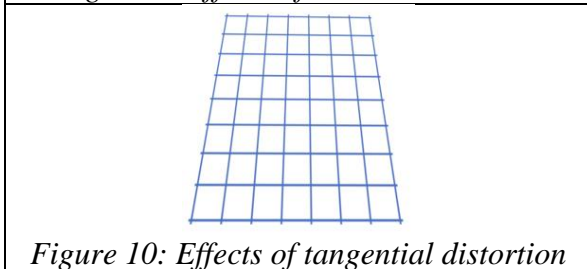


Figure 10: Effects of tangential distortion

The extrinsic camera parameters have six degrees of freedom that describe the position of the camera in the “world” (three translations and three rotations) and the intrinsic parameters K has five degrees of freedom, a total of 11 degrees of freedom. Equation 1 describes the correspondence between 3D world points X and 2D pixel locations of an undistorted image x , which can also be written as equation 3:

$$x = PX, \quad 3$$

where $P = K[R \ t]$ and is called the “camera matrix”. For a general projective camera, the camera matrix P is given by equation 4, where p_{34} is always equal to 1. Therefore, P has 11 degrees of freedom and a matrix rank of 3[11].

$$P = \begin{bmatrix} p_{11} & p_{12} & p_{13} & p_{14} \\ p_{21} & p_{22} & p_{23} & p_{24} \\ p_{31} & p_{32} & p_{33} & p_{34} \end{bmatrix}. \quad 4$$

b) Camera-projector calibration

There are many commercial and open source software that can achieve a single or stereo camera calibration, however there are only a handful of research efforts that describe the calibration of a camera and a projector [13,14,15]. These research efforts throw light on the ways a scanner manufacturer may approach the process of calibrating an instrument. We briefly describe one such method to perform a camera-projector calibration.

The primary reason to perform the camera-projector/scanner calibration is to reduce the average reprojection error. Reprojection error is defined as the average of the distance between points projected to the camera's image plane using the camera parameters (intrinsic, extrinsic and distortion) and the points captured by the camera. It is the correction needed to obtain a near-perfect correspondence between the projected and the captured images [9]. This reprojection error convolves all the intrinsic, extrinsic, radial, and tangential distortion parameters of both the projector and the camera. Lower reprojection errors indicate a better estimate of the camera parameters. Once calibrated, the intrinsic parameters are typically constant for an SL scanner. This assumes that the projector's focus and magnification settings are constant, and the camera's settings for focal length and aperture are constant. The camera's settings can be maintained constant by disabling any automatic settings and enabling a manual mode.

The extrinsic parameters of an SL scanner can change if the relative position or orientation between the camera and the projector is changed due to intentional or accidental mechanical movement. To simplify the calculations in our implementation, once the SL scanner was calibrated, the “world” origin was arbitrarily set to either the camera's origin or the projector's origin. In this case, the rotation and translation parameters then referred to those between the camera and the projector. The extrinsic parameters between the camera and the projector can be maintained constant by using rigid mounting apparatus for both the camera and the projector. If these conditions are not met, the system must be recalibrated before every scan.

The custom-built SL scanner (SC) uses a calibration routine [14] and needs at least three sets of data, with each dataset consisting of multiple images of the grid plate in different positions that are used for camera calibration first and then the scanner calibration. More positions will lower the reprojection error. To understand the sources that dominate the reprojection error, 14 calibration datasets were obtained and three datasets at a time were processed using scanner SC's calibration routine. The reprojection errors of the camera, projector, and the scanner (stereo) are shown in Figure 11a. It may be observed that the stereo component dominates the camera or the projector reprojection error. Both the camera and projector reprojection errors have low mean values and low variability compared to the stereo reprojection errors. When the same process was

repeated, now using 13 datasets at a time, the stereo calibration error reduced considerably and is shown in Figure 11b.

The intrinsic parameters from the calibration are given in Table 3. The units of f_x , f_y , c_x , c_y , s and the reprojection error (e_R) are pixels and k_1 , k_2 , k_3 , p_1 , p_2 are the radial and tangential distortion parameters that are dimensionless. Only 75 dataset combinations of the possible 364 ($^{14}C_3$) were considered to calculate the statistics for Table 3a and the calibration routine failed to calculate the parameters for one of the 14 possible combinations in Table 3b. From both Table 3 and Figure 11, it is evident that using more calibration datasets is beneficial in lowering the bias and

Table 3: One standard deviation values of the intrinsic, extrinsic and distortion parameters of the custom-built scanner

	Camera	Projector		Camera	Projector
f_x	46.685	154.455	f_x	1.633	13.463
f_y	39.196	117.146	f_y	1.411	9.448
c_x	4.375	32.348	c_x	0.905	2.754
c_y	41.470	127.601	c_y	1.552	18.195
s	0.000	0.000	s	0.000	0.000
k_1	0.009	0.093	k_1	0.001	0.005
k_2	0.012	1.304	k_2	0.003	0.007
p_1	0.001	0.006	p_1	0.000	0.000
p_2	0.002	0.004	p_2	0.000	0.001
k_3	0.000	0.000	k_3	0.000	0.000
e_R	0.020	0.054	e_R	0.004	0.011

a) Calibration using 3 datasets at a time

b) Calibration using 13 datasets at a time

variation in the reprojection errors, but also that the projector's intrinsic parameters have higher bias and variation than that of the camera. This is to be expected since the projector's optics are typically of lower quality than that of a camera.

The reprojection error affects the measurements such as sphere-to-sphere distance etc. A reprojection error less than 0.1 pixel is considered acceptable in practice, however, obtaining a correlation between the reprojection error and error in measuring an artifact (say a dumbbell) is not trivial. This is because, larger reprojection errors distort the 3D point cloud data to such an

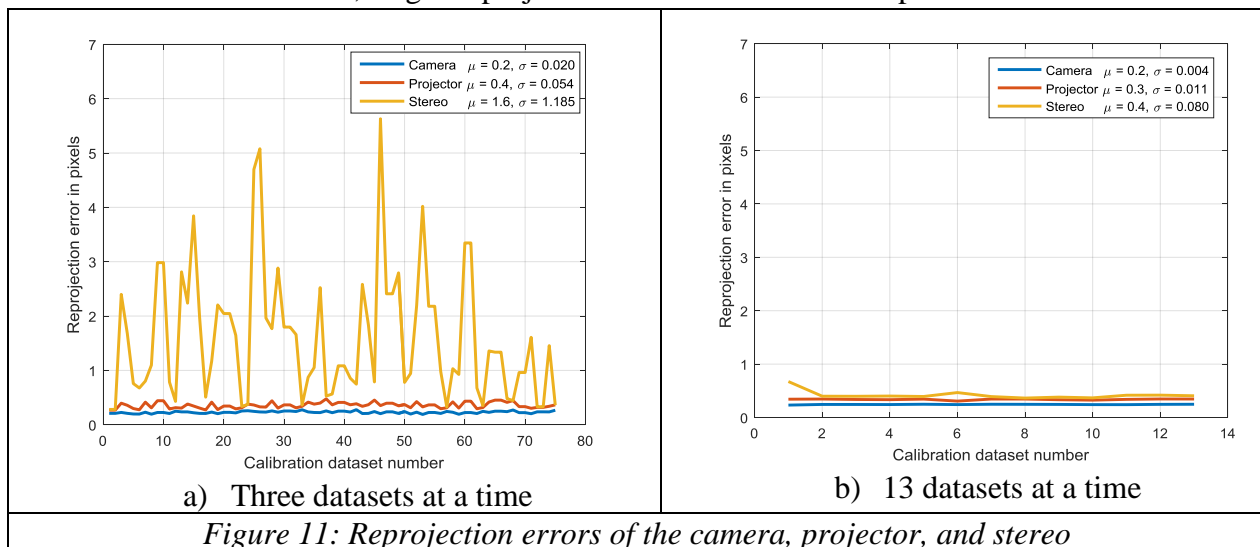
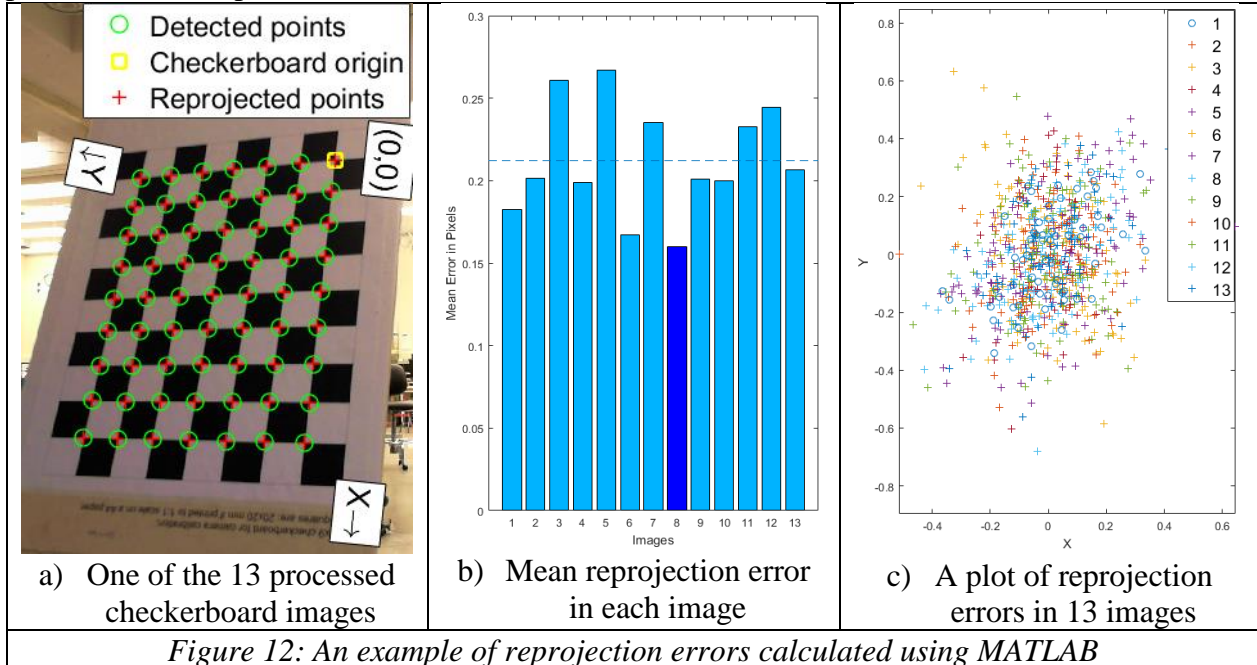


Figure 11: Reprojection errors of the camera, projector, and stereo

extent that the scan of a sphere does not appear to be a sphere. However, the distance (d_{CP}) between the camera and the projector of the custom-built scanner (SC) was calculated from the translation component of the extrinsic parameters (stereo). This distance (d_{CP}), correlated well with the reprojection error (e_R) in multiple calibration routines and the correlation coefficient was 0.85.

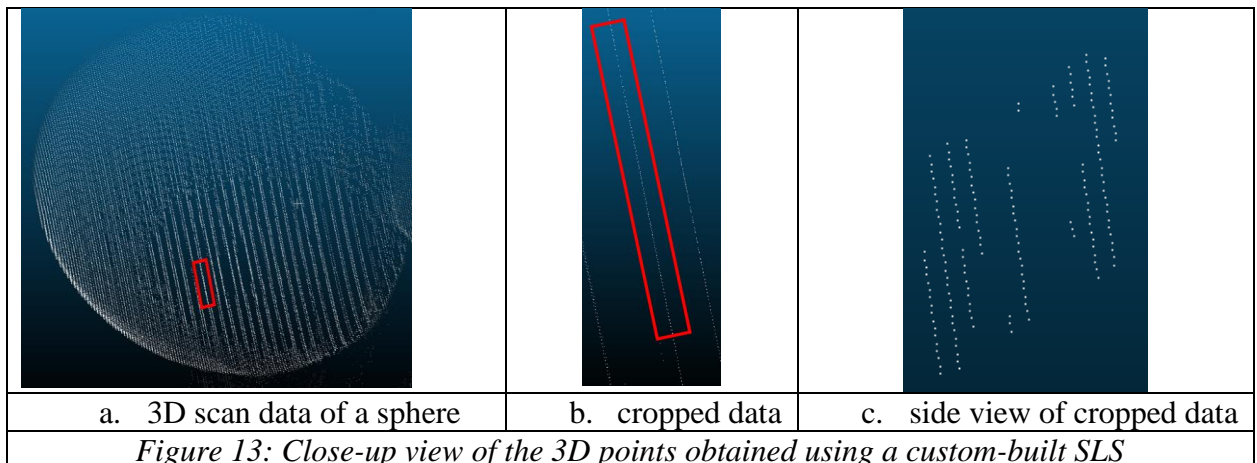
5.1.2 Calibration artifact

The calibration artifact recommended by many software suites is a pattern of images on a flat plate. These patterns could be anything that can be easily detected by the image processing software and are typically 2D checkerboard patterns or circular patterns. These patterns can be easily printed on a paper using a laser printer and adhered to a rigid plate. However, most software assume that the grid pattern is uniform, and that the flatness of the pattern is zero. If the flatness is large, or if the laser printer has a scaling/skew error, it will increase the reprojection error. Figure 12 shows an example of the reprojection errors calculated by MATLAB using a calibration pattern printed on a laser printer.



5.1.3 Camera and projector resolution

In an ideal scanner, a single coded line projected by a projector is imaged by a camera and the line's image is exactly one pixel wide. Alternatively, the projected line in the structured pattern itself may be intentionally wider. However, when the pixel resolution of the projector and camera vary, it might result in redundant points. These points are typically away from the object's surface along the line joining the camera and the pattern's projection location on the object.



To explain this effect, let us assume that a single line projected by a projector is captured by a camera as a distorted line that is 10 pixels wide. If the method of calculation of the 3D point involves a plane-point intersection, it will result in 10 points for a single coded line from the projector. These points must be filtered to get an accurate representation of the object. Figure 13 shows this issue using data obtained from a 100 mm diameter sphere at 0.67 m from scanner SC. Figure 13c shows the side view of the data in Figure 13b which appear to be penetrating the sphere surface. The missing points in Figure 13c could be a result of the lack of enough intensity of the pattern in the captured image. The points in Figure 13c were fit to a plane and the one standard deviation (1σ) value of the residuals was 5.8 nm – a negligible value. This indicates that these points are indeed redundant and may be filtered out.

5.1.4 Camera and projector's depth of field

Commercial DSLR cameras have variable apertures that enable a user to set the working distance and the depth of field (DOF), which is the distance between the nearest and the furthest part of an image that appears to be sharp. Knowledge of DOF is necessary to determine the scanning volume of an SL scanner. Larger DOF ensures that the images of the patterns captured are sharp resulting in lower noise. Figure 14 shows the variation of the DOF with varying aperture diameter for one DSLR camera.

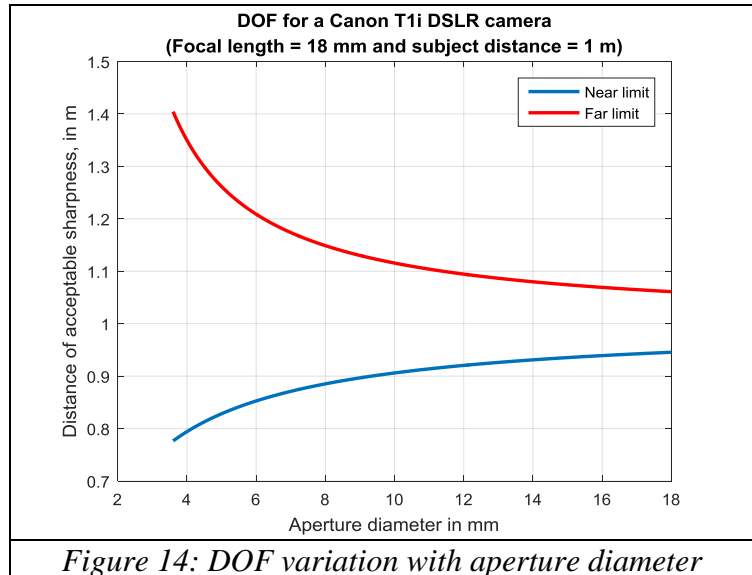


Figure 14: DOF variation with aperture diameter

Projectors on the other hand have a very narrow DOF that cannot be adjusted, which limits the ability of the projector to project patterns with sufficient sharpness on the objects. Commercial projectors are designed to output the maximum amount of light without any hinderance and therefore do not have any aperture control and consequently have limited DOF.

The projector used for scanner SC has a narrow DOF of ≈ 50 mm that was measured by visual observation of projected image sharpness, whereas the artifacts measured using the scanner are of 100 mm in diameter, placed at distances over 100 mm from one another. There are several methods to enhance the DOF of such projectors in open literature. One such method is described by Iwai et al [16], that uses an electrical focus tunable lens (FTL) in front of projector's objective to increase its DOF. However, it is not clear if any of the commercial scanners are using any specific methods to enhance the DOF of projectors.

5.1.5 Triangulation angle/configuration

Since the principle of an SL scanner is based on triangulation, the measurements are affected by the angle θ between the camera, the object and the projector (illustrated in Figure 15). The measurement is also affected by the distance between the camera and the projector, b , and the distance between the camera and the object, d . The relationship between the parameters in this setup is given by equation 5 [17]. When $\theta \approx 0^\circ$, $\alpha + \beta \approx 180^\circ$ and $b \approx 0$. This will result in large errors due to uncertainty in calculating the depth d . When $\theta \approx 90^\circ$, the camera may not capture any useful image of the pattern and can be impractical when measuring deep features or holes. A typical arrangement involves keeping the angle $\theta \approx 30^\circ$.

$$d = b \left(\frac{\sin(\alpha)}{\sin(\alpha + \beta)} \right)$$

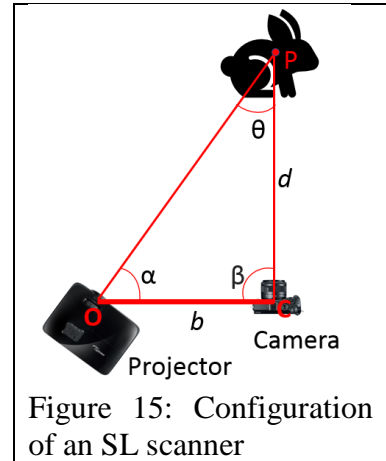


Figure 15: Configuration of an SL scanner

5

5.1.6 Coding techniques

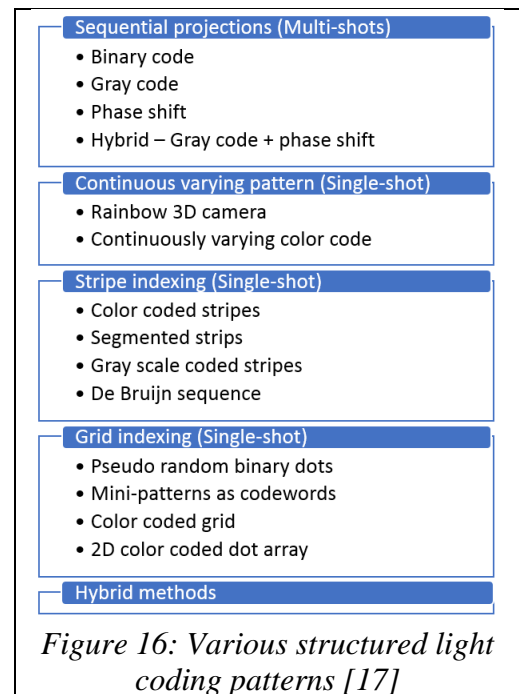
Geng [17] details a variety of techniques to code the light patterns, which include temporal (multi-shot/sequential) and spatial (single-shot) techniques. Multi-shot techniques are useful when the object being scanned is stationary, and results in more accurate measurements than single-shot techniques. Coding techniques affect the performance of the scanner [18] and each of these techniques have their specific applications, advantages, and disadvantages. Many scanners do not offer a way to change the light pattern coding and scanners are optimized for certain kinds of applications such as industrial metrology, gaming or dentistry.

5.1.7 Wavelength/Color of light for monochromatic coding patterns

Some of the latest commercial structured light scanners use a blue light source. Some manufacturers claim that this type of light source reduces errors due to ambient lighting and reduces reflections due to short wavelength. Blue light is useful for some applications like scanning skin and teeth for dental applications [19]. While using blue light, the hardware and software allow the scanner to filter out ambient light and obtain higher quality scans. It is, however, not well understood if blue light scanners offer any significant advantage over white, or any other color lighting for most other applications.

5.1.8 "Rainbow effect" in projectors

Certain digital light processing (DLP) projectors use a mechanical color wheel to generate sequential color. Such a color wheel can interfere with the coding techniques described earlier due to a visible color artifact known as the "rainbow effect"[20]. Coupled with the camera's exposure



time variation, the rainbow effect can result in measurement errors. The mechanism to rotate the disc may also cause the projector to vibrate and can cause errors in measurements.

5.1.9 Lamp temperature

Many projectors use halogen or metal halide lamps as their light source and their operating temperatures can be anywhere from 35 °C to 300 °C and can cause the scanner components to thermally move with respect to each other. Most instruments have a warm-up period that addresses this issue. The projector's lamp is a major heat source that can also affect the mounting apparatus and thereby affect the calibration parameters of the scanner. Some scanners offer projectors with LED light sources which operate at lower temperatures that mitigate this issue.

5.2 Errors due to target/artifact shape and optical/mechanical properties

The VDI/VDE 2634 guidelines recommend the use of spheres and flat plates that have diffusely scattering surfaces. These kinds of targets are known to offer near-lambertian surfaces that provide data with low noise. However, such surfaces may not always be found in practical applications. Most optical scanners perform poorly with shiny and/or dark surfaces. Scanning concave surfaces also is challenging for scanners with large triangulation angles.

5.3 Errors due to environment

5.3.1 Ambient lighting

Ambient lighting is one of the major sources of error that can affect the quality of the data. The reconstruction algorithm of the SL scanner relies on observing the pattern in the captured image which may be coded based on light intensity from the projector. For example, consider a binary code used to digitally paint an object with a line numbered '23' whose binary representation is '10111'. If a speckle of light from the environment alters the intensity of light and saturates the image captured by the camera, it will result in an image that is coded '11111' which in decimal is '31'. This will cause an error in calculation of the depth using triangulation. However, in practice, it is typical to use intensity thresholding to exclude pixels that do not fall between certain preset intensities, which will result in missing points in 3D data. We also observed that some scanner manufacturers compensate for ambient lighting that mitigates this issue.

5.3.2 Ambient Temperature

Ambient temperature variation is an important source of error in many dimensional measurements. If the instrument is calibrated at one temperature and is used to measure an object at a different temperature, the measurement may be erroneous due to the lack of mechanical stability within the temperature range.

5.3.3 Other environmental factors

Factors such as humidity, fingerprints, smudges, and dust can result in the optics getting fogged up and/or dirty resulting in measurement errors.

5.4 Errors due to mode of operation

SL scanners have several controllable parameters that are designed to generate a scan that is optimal for the target. The level of control to acquire scans varies with the instrument type and manufacturer. Parameters such as exposure time, gain, aperture diameter and exposure bracketing can result in datasets that have varying levels of noise. Not all scanner manufacturers offer a way to control these parameters, leading to the inability of an end user to compare scanners.

5.5 Errors due to data acquisition and post processing

Errors in characterizing SL scanners can also occur due to the way the scanner acquires data and the methods used to process the acquired data. Some of these issues are described in the following sub-sections.

5.5.1 Data acquisition and/or digitization

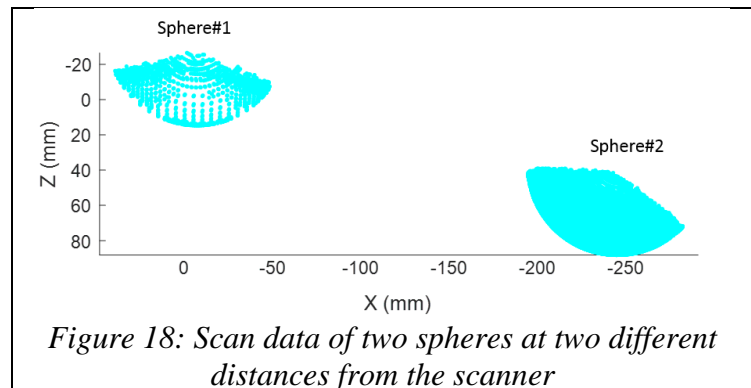
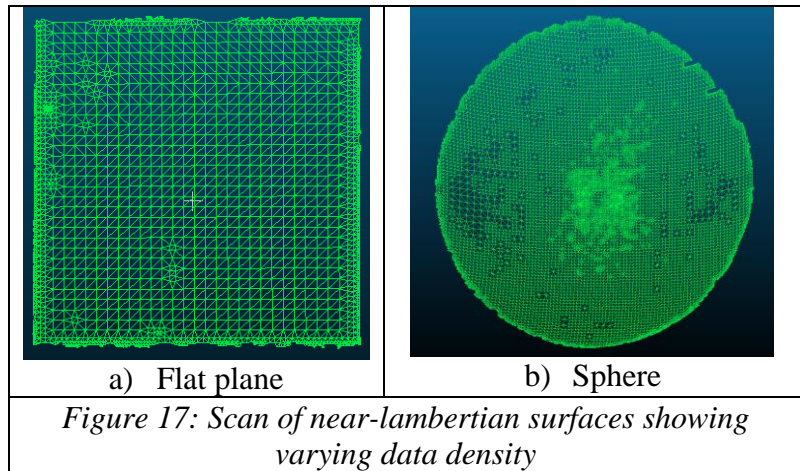
Data obtained from SL scanners is typically noisy and some data filtering must be performed to exclude data that

does not represent the object. Software provided by the scanner manufacturers typically use proprietary methods to perform some level of filtering. Figure 17 shows a scan of a flat aluminum plate and a sphere, both of which have bead-blasted and diffused surfaces. It was observed that the data density over the surface varies. The data density is higher along the edges and at locations that have slightly higher reflectivity than the rest of the surface. Processing datasets that have non-uniform point density results in errors while calculating quality of parameters such as plane flatness, sphere diameter and form errors. It is also not clear whether these datasets were natively generated as a polygonal mesh or as 3D point cloud data.

5.5.2 Post-processing

Care must be taken while applying data filters in post-processing, as rejection of valid points or inclusion of invalid points will indirectly affect the performance results of the instrument. Structured light scanners produce varying point densities in the scanner work volume based on the location and orientation of the object surface. Two kinds of tests were performed that will show the effect of point cloud processing on scanner errors.

The first test was conducted by scanning two spheres, 15 times, at two distances from scanner SA as shown in Figure 18. Scan data of Sphere#1 had an average of 1465 points and Sphere#2 had an average of 13546 points. The average error in radius for Sphere#1 was 1.1 μm and that for Sphere#2 was 0.3 μm . Both the spheres were very similar in construction but resulted in different values for the error in radius. This was due to the varying point density and/or the location of the sphere in the scanner work volume.



A second test was conducted by scanning a square flat plane of 150 mm width at 10 different angles, and five repeat scans were obtained at each angle. This data was fit to a plane and the root-mean-square (RMS) value of the residuals was obtained and shown in Figure 19. This resulted in lower RMS noise of its residuals and the number of points scanned were lowered when the angle of rotation exceeded 15° to the scanner's XY plane. It should be noted here that the scanner's coordinate system was centered at the instrument work volume, the Z axis was away from the scanner in the horizontal plane and the XY plane is oriented vertically and not parallel to either the camera's image plane or the projector's sensor plane.

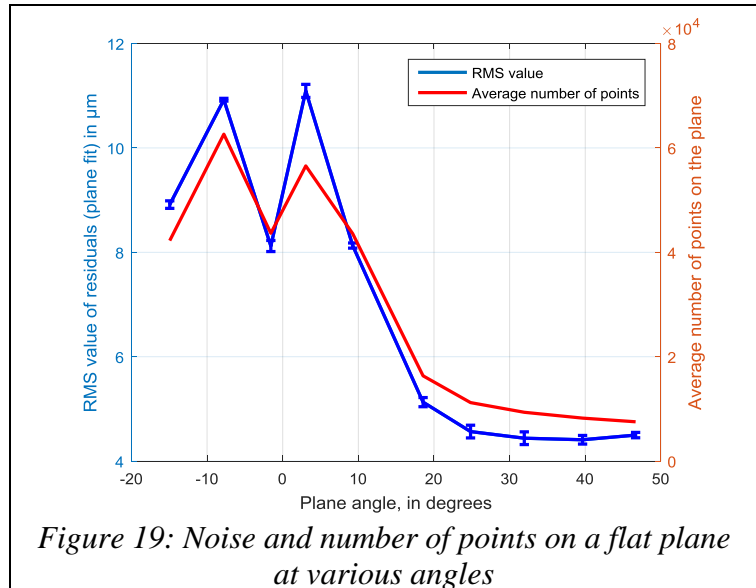


Figure 19: Noise and number of points on a flat plane at various angles

6 SUMMARY & FUTURE WORK

Structured light scanners are increasingly being used in many industrial applications. Several organizations are procuring these scanners based on limited understanding of their performance and a lack of adequate standards. Some guidance is provided by the VDI/VDE 2634 guidelines, but these guidelines need to be extended to encompass various kinds of SL scanners that are currently available.

DMG at NIST has started to explore these scanners by first understanding the sources of errors in the scanners and their effect on dimensional measurements. There are several error sources described in this paper that extend beyond the mathematical model of the scanner. The effect of each of these sources of errors on the quality parameters described in VDI/VDE 2634 guidelines is not well understood. Future activities are planned to identify the quality factors that are sensitive to these error sources and develop test procedures based on such information. The authors also plan to work with the ISO and other U.S. standards development organizations to develop new and fair performance evaluation tests that will improve commerce.

7 DISCLAIMER

Commercial equipment and materials may be identified to specify certain procedures. In no case does such identification imply recommendation or endorsement by the NIST, nor does it imply that the materials or equipment identified are necessarily the best available for the purpose.

8 ACKNOWLEDGEMENTS

The authors would like to thank the following experts and researchers for their valuable time, feedback and useful discussions: Dr. Craig Shakarji, Dr. Steve Phillips and Ms. Geraldine Cheok of NIST; Dr. Octavio Icasio Hernández of CENAM; Dr. Gabriel Taubin of Brown University; Mr. Luc Cournoyer of NRC-Canada; Mr. John Palmateer; Mr. Sean Woodward of NPL-UK; Dr. Michael McCarthy of Engineering Metrology Solutions – UK.

9 REFERENCES

- [1] VDI-Standard: VDI/VDE 2634 Blatt 2: https://www.vdi.eu/guidelines/vdivde_2634_blat_2-optische_3_d_messsysteme_bildgebende_systeme_mit_flaechenhafter_antastung/
- [2] VDI-Standard: VDI/VDE 2634 Blatt 3: https://www.vdi.eu/guidelines/vdivde_2634_blat_3-optische_3_d_messsysteme_bildgebende_systeme_mit_flaechenhafter_antastung/
- [3] Taubin, G., Moreno, D., Lanman, D, "The Laser Slit 3D Scanner" <http://mesh.brown.edu/desktop3dscan/ch4-slit.html> (Accessed on 11/23/2018)
- [4] El-Hakim S., Beraldin J., Blais, F., "Comparative evaluation of the performance of passive and active 3D vision systems", Proceedings Volume 2646, Digital Photogrammetry and Remote Sensing, December 1995. <https://doi.org/10.1117/12.227862>
- [5] MacKinnon, D., Beraldin, J., Cournoyer, J., Carrier, B., "Hierarchical characterization procedures for dimensional metrology," Proc.SPIE 7864, Three-Dimensional Imaging, Interaction, and Measurement, 786402 (27 January 2011); <https://doi.org/10.1117/12.872124>
- [6] Beraldin, J., Carrier, B., MacKinnon D., Cournoyer, L., "Characterization of Triangulation-based 3D Imaging Systems using Certified Artifacts", NCSLI Measure, 7:4, 50-60, <https://doi.org/10.1080/19315775.2012.11721620>
- [7] McCarthy, M., Brown, S., Evenden, A., & Robinson, A., "NPL freeform artefact for verification of non-contact measuring systems", Proc.SPIE 7864, Three-Dimensional Imaging, Interaction, and Measurement, 786402 (27 January 2011); <http://doi.org/10.1117/12.876705>
- [8] Taubin, G., Moreno, D., Lanman, D, "3D Scanning with Structured Light" <http://mesh.brown.edu/desktop3dscan/ch5-structured.html> (Accessed on 11/23/2018)
- [9] Zhang, Z., "A flexible new technique for camera calibration", IEEE Transactions on Pattern Analysis and Machine Intelligence, 22(11), Nov 2000. <https://doi.org/10.1109/34.888718>
- [10] Bouget, J., "Camera Calibration Toolbox for MATLAB", http://www.vision.caltech.edu/bougetj/calib_doc/ (Accessed 2/12/2019)
- [11] Hartley, R., Zisserman, A., "Multiple View Geometry in Computer Vision", 2nd edition, Cambridge University Press New York, NY, USA, 2003 ISBN:0521540518
- [12] Bradski, G., Kaehler, A., "Learning OpenCV: Computer Vision with the OpenCV Library", O'Reilly Media, Inc., 2013, ISBN:9780596516130 pp 373,376
- [13] Falcao, G., Hurtos, N., Massich, J., Fofi, D., "Projector-Camera Calibration Toolbox", <https://github.com/davidfofi/procamcalib.git>, 2009.
- [14] Moreno, D., and Taubin, G., "Simple, Accurate, and Robust Projector Camera Calibration", In 3DIMPVT, pp. 464–471, 2012

- [15] Huang, B., Ozdemir, S., Tang, Y., Liao, C., Ling, H. "A Single-shot-per-pose Camera-Projector Calibration System for Imperfect Planar Targets", 2018 <https://arxiv.org/pdf/1803.09058.pdf>
- [16] Iwai D., Mihara S., Sato K., "Extended Depth-of-Field Projector by Fast Focal Sweep Projection", IEEE Transactions on Visualization and Computer Graphics, 21 (4), Apr 18, 2015.
- [17] Geng J., "Structured-light 3D surface imaging: a tutorial," Adv. Opt. Photon. 3, 128-160 (2011) <https://doi.org/10.1364/AOP.3.000128>
- [18] Salvi, J., Pages, J., Batlle, J., "Pattern Codification Strategies in Structured Light Systems", Pattern Recognition, Vol 37, Issue 4, April 2004.
- [19] Jeon, J., Choi, B., Kim, C., Kim, J., Kim, H., Kim, W., " Three-dimensional evaluation of the repeatability of scanned conventional impressions of prepared teeth generated with white- and blue-light scanners", The Journal of Prosthetic Dentistry, 114 (4), Oct 2015.
- [20] Baker, M., Xi, J., Chicharo, J., Li, E., "A contrast between DLP and LCD digital projection technology for triangulation-based phase measuring optical profilometers", Proceedings Volume 6000, Two- and Three-Dimensional Methods for Inspection and Metrology III; 60000G (2005) <https://doi.org/10.1117/12.632582>